

Note: Sensitive fluorescence detection through minimizing the scattering light by anti-reflective nanostructured materials

Supeng Xu,¹ Yanning Yin,¹ Ruoxi Gu,¹ Meng Xia,¹ Liang Xu,¹ Li Chen,² Yong Xia,^{1,3,a)} and Jianping Yin¹

¹Key Laboratory of Precise Spectroscopy, School of Physics and Materials Science, East China Normal University, Shanghai 200062, People's Republic of China

²Shanghai Key Laboratory of Green Chemistry and Chemical Processes, School of Chemical and Molecular Engineering, East China Normal University, Shanghai 200062, People's Republic of China

³Collaborative Innovation Center of Extreme Optics, Shanxi University, Taiyuan, Shanxi 030006, People's Republic of China

(Received 20 November 2017; accepted 22 March 2018; published online 4 April 2018)

We demonstrate a new approach with fabrication of anti-reflective coating to substantially reduce the scattering light in an ultra-high vacuum during laser induced fluorescence (LIF) detection. To do so, the surface of the vacuum chamber in the detection region was blackened and coated with the special solar heat absorbing nanomaterials. We demonstrate that more than 97.5% of the stray light in the chamber spanning from near infrared to ultraviolet can be absorbed which effectively improves the signal to noise (S/N) ratio. With this technique, the LIF signal from the cold magnesium monofluoride molecules has been observed with an S/N ratio of ~4 times better than without that. *Published by AIP Publishing.* <https://doi.org/10.1063/1.5016566>

Precision fluorescence spectroscopy plays an increasingly important role in the areas such as the precision measurement of fundamental physical constants,¹ single-molecule microscopy,² single-ion quantum dynamics,³ the search for the electron's electric dipole moment,⁴ and direct laser cooling of molecules.^{5,6} The laser-induced fluorescence technique is widely used in the study of the electronic excitation of atoms (or molecules, ions) and their interactions with other species.⁷ Generally, the signal-to-noise (S/N) ratio of the fluorescence signal from excited atoms or molecules can be very high, leading to the sufficient sensitivity for measurements conducted. However, in some challenging experiments, the laser induced fluorescence (LIF) signal is fairly small. For example, in the gas phase, rovibrational branching from molecular electronic states may deliver the LIF signal smaller than one photon per molecule.⁸ When a small quantity of molecules is detected with the quite weak signal, the scattered laser light can seriously contribute to the big and unwanted noise. In the laser cooling of Yb: ZBLAN solids,⁹ most of the pump laser radiation is eventually absorbed by the Yb³⁺ ions in the glass while ideally the fluorescence emitted should be absorbed as much as possible by the chamber walls. This is because the fluorescence may re-pump the cooling crystals, causing it to be heated through a Stokes process. Therefore, it is very critical for these types of LIF experiments to minimize the unnecessary scattering light so that a better S/N ratio can be obtained.

Coated surfaces in black are often used to absorb the scattered light during fluorescence detection. Chemically grown black cupric oxide materials have been used for stray light suppression, and the efficient LIF detection of the SrF molecules

has been achieved.⁸ In that experiment,⁹ the cooling crystal is closely surrounded by a copper chamber coated with low-thermal-emissivity materials, but the coating materials absorb sufficiently the emitted photons at the fluorescence wavelengths, so the radiative load is reduced by a factor of six. Some surface topography methods have also been developed with the anti-reflective coating (ARC) nanostructures through coated surfaces. Both silicon and non-silicon materials along with their mechanisms responsible for reflectance reduction are reviewed.^{10–14}

Here, we present a succinct experimental scheme to minimize the stray light for our diatomic molecule laser cooling experiments. The special solar heat absorbing materials we chose were sprayed evenly on the interior surface of the stainless steel vacuum chamber where the LIF experiments were performed.¹⁵ With this micron-thickness coating, we demonstrate a number of benefits, i.e., low light reflectance, high thermal stability, excellent adhesion, broad spectral absorption region, and low outgassing. The fabrication procedures of the anti-reflective coating materials are as follows. First, vacuum chamber components were cleaned in an ultrasonic bath that is filled with acetone for 1 h to remove any surface contamination, followed by a rinse in a deionized water bath. They were then placed in an oven at 50 °C for 10 min to obtain a dry surface. Because this coating is soluble in water, ensure that the surface is dry before spraying. Afterwards, we used a spray gun with 1.5 mm aperture to blacken the surface of the components. The vacuum chamber was coated through six vents, each of which was sprayed for 10 s. Then we put the components in the drying oven at 70 °C. Twenty minutes later, we carry out the second layer of spraying. Finally, the components were placed in the drying oven at the same temperature for 12 h so that any volatile substances can evaporate as completely as possible.

^{a)}Author to whom correspondence should be addressed: yxia@phy.ecnu.edu.cn.

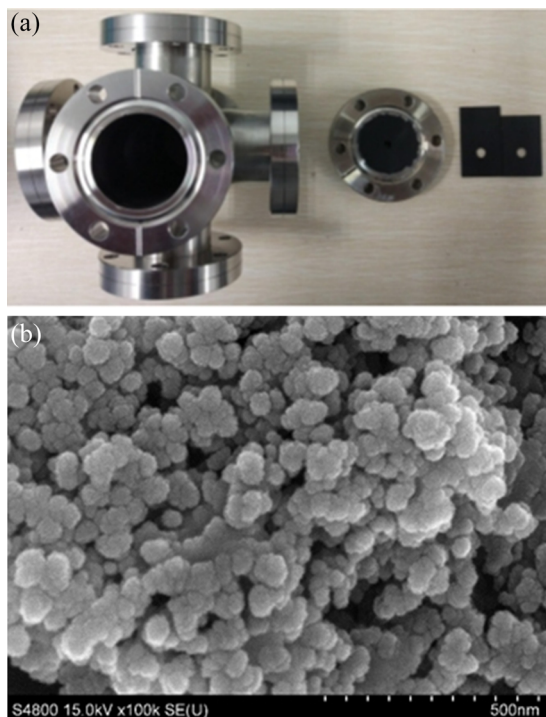


FIG. 1. (a) Coated vacuum chamber, flange, and sheet samples. (b) Scanning electron micrograph photograph for a small area of the coated surfaces.

The coated components are showed in Fig. 1(a). They consist of a vacuum chamber, a flange, and sheet samples. A scanning electron micrograph for a portion of the coated areas is shown in Fig. 1(b). A visual observation of the coated structure reveals the granular and porous structure that attests for the anti-reflection properties. From the surface area spectrum taken by the microscope, the relatively uniform spherical nanoparticles of 50–80 nm diameters are visible. The average depth of the coated layers is micron size. We continue to bake the coated components to 150 °C for 4 h, and the coating material still shows high thermal stability and excellent adhesion. The main ingredients of the coating materials are resin, nanoceramic powder, and carbon powders. The ultimate pressure of the vacuum chamber was measured to be near 3.5×10^{-9} Torr with the surface coating.

The porous structures of these nanoparticles on the chamber's surface are found to efficiently trap the scattering light in our experiments. To quantify the extent of the reduction for the scattering light background due to the material's coating, we measured the stray light signal under the atmospheric environment with the coated vacuum chamber and the same

chamber but without coating. For an exhaustive comparison, we directed a laser beam with a $1/e^2$ diameter of 1 mm to both of the centers of front and rear windows of the chambers and adjusted the laser power with a wavelength plate. A chopper wheel modulated the incident laser light at 700 Hz, and the scattering light was collected by a photomultiplier tube (PMT) and then transmitted to a lock-in amplifier to integrate with the reference signal. The scattering light noise signal can be extracted by adjusting their phase difference. A fraction of the laser beam was picked up by a photodetector to account for the laser power fluctuation; the fluctuation was smaller than 1% of the incident laser light power throughout the measurements. The specific measurement scheme is seen in Fig. 2. Here, we define the absorption efficiency as $A = 1 - (P_c/P)$, where P_c and P are the signal intensity from the PMT with and without the coated surfaces, respectively.

In Fig. 3, we show the measured absorption efficiency from the coated chamber at a wavelength of 359 nm with a laser power up to 25 mW. In general, the measured efficiency is constant, 97.5%, as seen in Fig. 3 (the dotted line). The inset is the stray light intensity collected by the PMT versus incident laser power. We see that the stray light signal from the PMT remains linear with and without the coatings. For the experiments with the higher laser power, the same trend can also be obtained when a neutral density filter is placed in front of the PMT detector to avoid signal saturation.

In order to investigate the coating response to the wavelength, we measured the absorption efficiency from near infrared to ultraviolet band. For each data point, we measured the absorption efficiency of the 5, 10, and 15 mW power laser, respectively, and then averaged. In the visible light bands, the absorption efficiency by the coating is excellent, as seen in Fig. 4, especially at 400 nm, 518 nm, 633 nm, and 673 nm, exceeding 99%. From 700 to 820 nm, we used a Ti:sapphire laser and acquired the data points. The measured absorption efficiency by the coating is above 98%. Note that 359 nm is near the laser cooling wavelength for our magnesium monofluoride (MgF) molecules.^{16,17} Although the absorption efficiency is not as high, it is still more than 97.5%. In short, the solar heat absorbing coating material is effective in reduction of the unwanted stray light.

Now, we move to our preliminary experiments on laser cooling of diatomic molecules. A pulsed laser (YAG 20–22 mJ, 5 ns, 532 nm, 2 Hz) ablated an Mg rod in a 5 K copper cell where 4 SCCM of precooled 5 K helium and 0.05 SCCM of 230 K SF₆ flowed in.¹⁸ The Mg and SF₆ react to create MgF molecules which are cooled by collisions with He and leave the cell through a 5 mm aperture. The resulting pulse passes

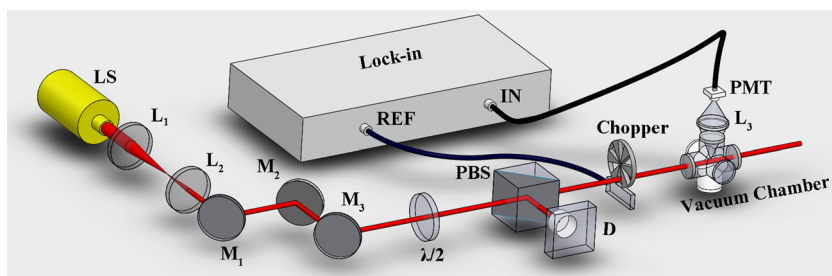


FIG. 2. Schematics to measure the high absorption efficiency of stray light by the coating. LS: laser source; L: lens; M: mirror; PBS: polarizing beam splitter; D: photodetector; PMT: photomultiplier; Lock-in: lock-in amplifier; $\lambda/2$ is half-wave plate.

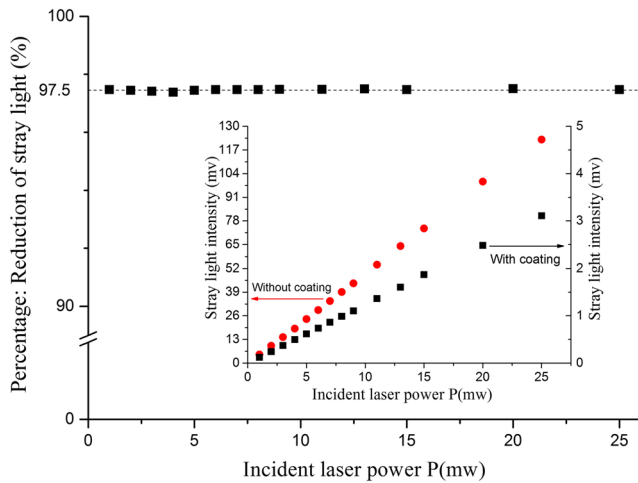


FIG. 3. Reduction of the stray light vs the incident laser power. The inset is the absolute signal intensity collected by the PMT versus incident laser power.

through a 5 mm diameter aperture, 12 cm downstream, where the pressure is 3×10^{-9} Torr. Then the molecular beam passes two detection regions, 30 and 40 cm from the exit of the source, respectively, where the chambers are all the same except for the ARC. Although they have different molecular density (at different distances), we care more about the background stray light, which is mainly caused by the scattering of the probe light, than the fluorescence signal. A beam of probe laser was split into two with a beam splitter, and two attenuators were used to adjust their light intensity to 2 mW. By exciting the $X^2\Sigma^+_{1/2}(v=0) \rightarrow A^2\Pi_{1/2}(v'=0)$ electronic transition (359.2 nm),¹⁷ we used two calibrated PMTs to collect the signal at the same time. A gated photon counting systems processes the fluorescence signal, and a variable time delay pulse opens an adjustable “window” in the photon counting system after the YAG laser is triggered. To increase the signal intensity, multiple rounds of signals are accumulated. In Fig. 5, we show the LIF signals for the MgF experiments. So, the addition of the coated surfaces significantly eliminates the scattering light. The maximum S/N ratio is then enhanced by a factor of ~ 4 .

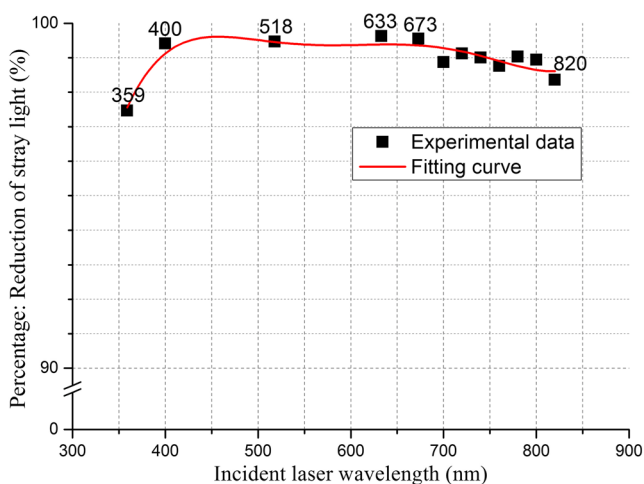


FIG. 4. Reduction of the stray light as a function of the incident laser wavelength.

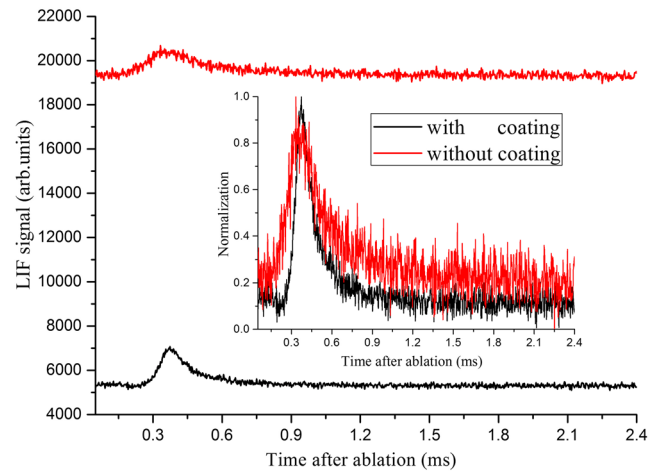


FIG. 5. LIF measurements for MgF molecules produced in a buffer gas cooling. Black and red curves refer to the coating and without coating, respectively.

In conclusion, with the coating of the new materials onto the surfaces of the LIF detection chambers, we succeed in achieving the lower noise from the stray light for the ongoing LIF experiments of cooling diatomic molecules. The coated surfaces have high absorption efficiency for the stray light from 359 nm to 820 nm. The approach presented here is widely suitable to reduce the scattered light background in any other similar LIF experiments where only a low concentration of exotic molecules can be produced.

We acknowledge support from the National Natural Science Foundation of China under Grant Nos. 91536218 and 11374100, and the Natural Science Foundation of Shanghai (Grant No. 17ZR1443000).

- ¹J. Biesheuvel, J. P. Karr, L. Hilico, K. S. E. Eikema, W. Ubachs, and J. C. J. Koelemeij, *Nat. Commun.* **7**, 10385 (2016).
- ²W. E. Moerner and D. P. Fromm, *Rev. Sci. Instrum.* **74**, 3597 (2003).
- ³D. Leibfried, R. Blatt, C. Monroe, and D. Wineland, *Rev. Mod. Phys.* **75**, 281 (2003).
- ⁴J. J. Hudson, D. M. Kara, I. J. Smallman, B. E. Sauer, M. R. Tarbutt, and E. A. Hinds, *Nature* **473**, 493 (2011).
- ⁵E. S. Shuman, J. F. Barry, and D. DeMille, *Nature* **467**, 820 (2010).
- ⁶S. Truppe, H. J. Williams, M. Hambach, L. Caldwell, N. J. Fitch, E. A. Hinds, B. E. Sauer, and M. R. Tarbutt, *Nat. Phys.* **13**, 1173 (2017).
- ⁷J. L. Kinsey, *Annu. Rev. Phys. Chem.* **28**, 349 (1977).
- ⁸E. B. Norrgard, N. Sitaraman, J. F. Barry, D. J. McCarron, M. H. Steinecker, and D. DeMille, *Rev. Sci. Instrum.* **87**, 053119 (2016).
- ⁹D. V. Seletskiy, S. D. Melgaard, S. Bigotta, A. Di Lieto, M. Tonelli, and M. Sheik-Bahae, *Nat. Photonics* **4**, 161 (2010).
- ¹⁰S. Chattopadhyay, Y. F. Huang, Y. J. Jen, A. Ganguly, K. H. Chen, and L. C. Chen, *Mater. Sci. Eng.: R: Rep.* **69**, 1 (2010).
- ¹¹Y. F. Li, J. H. Zhang, and B. Yang, *Nano Today* **5**, 117 (2010).
- ¹²H. K. Raut, V. A. Ganesh, A. S. Nair, and S. Ramakrishna, *Energy Environ. Sci.* **4**, 3779 (2011).
- ¹³L. Yao and J. H. He, *Prog. Mater. Sci.* **61**, 94 (2014).
- ¹⁴J. G. Cai and L. M. Qi, *Mater. Horiz.* **2**, 37 (2015).
- ¹⁵The solar heat absorbing material (Model RLHY-2337) is from Rongli-hengye Corporation.
- ¹⁶Y. N. Yin, Y. Xia, X. J. Li, X. X. Yang, S. P. Xu, and J. P. Yin, *Appl. Phys. Express* **8**, 092701 (2015).
- ¹⁷L. Xu, Y. N. Yin, B. Wei, Y. Xia, and J. P. Yin, *Phys. Rev. A* **93**, 013408 (2016).
- ¹⁸X. J. Li, L. Xu, Y. N. Yin, S. P. Xu, Y. Xia, and J. P. Yin, *Phys. Rev. A* **93**, 063407 (2016).